Development of high spatial resolution annual emission inventory of greenhouse gases from open straw burning in Northeast China from 2001 to 2020

Zihan Song[a,b], Leiming Zhang[c], Chongguo Tian[d], Qiang Fu[a,b], Zhenxing Shen[e], Renjian Zhang[f], Dong Liu[a,b], Song Cui[a,b*]

[a] *International Joint Research Center for Persistent Toxic Substances (IJRC-PTS), School of Water Conservancy and Civil Engineering, Northeast Agricultural University, Harbin, Heilongjiang, 150030, China*

[b] *Research Center for Eco-Environment Protection of Songhua River Basin, Northeast Agricultural University, Harbin, Heilongjiang, 150030, China*

[c] *Air Quality Research Division, Science and Technology Branch, Environment and Climate Change Canada, Toronto, Ontario, M3H 5T4, Canada*

[d] *CAS Key Laboratory of Coastal Environmental Processes and Ecological Remediation, Yantai Institute of Coastal Zone Research, Chinese Academy of Sciences, Shandong Key Laboratory of Coastal Environmental Processes, YICCAS, Yantai, 264003, China*

[e] *Department of Environmental Sciences and Engineering, Xi'an Jiaotong University, Xi'an, 710049, China*

[f] *Institute of Atmospheric Physics, Chinese Academy of Sciences, Beijing 100029, China*

*Corresponding author: Dr. Song Cui Email: cuisong-bq@neau.edu.cn (S. Cui)

WORD COUNT: 6000

7 FIGURES

1 TABLE

Abstract

Open straw burning has been widely recognized as a significant source of greenhouse gases (GHGs), posing critical risks to atmospheric integrity and potentially exacerbating global warming. In this study, we proposed a novel method that integrates crop cycle information into extraction and classification of fire spots from open straw burning in Northeast China from 2001 to 2020. By synergizing the extracted fire spots with the modified Fire Radiative Power (FRP) algorithm, we developed high spatial resolution emission inventories of GHGs, including carbon dioxide (CO_2), methane (CH_4), and nitrous oxide (N_2O). Results showed that the northern Sanjiang Plain, eastern Songnen Plain, and eastern Liao River Plain were areas with high intensity of open straw burning. The number of fire spots was evaluated during 2013-2017, accounting for 58.2% of the total fire spots observed during 2001-2020. The prevalent season for open straw burning shifted from autumn (pre-2016) to spring (post-2016), accompanied by a more dispersed pattern in burning dates. The two-decade cumulative emissions of CO_2, CH_4, and N_2O were quantified at 198 Tg, 557 Gg, and 15.7 Gg, respectively, amounting to 218 Tg of CO_2-eq. Significant correlations were identified between GHGs emissions and both straw yields and straw utilization ($p < 0.01$). The enforcement of straw burning bans since 2018 has played a pivotal role in curbing open straw burning, and reduced fire spots by 51.7% on annual basis compared to 2013-2017. The novel method proposed in this study considerably enhanced the accuracy in characterizing spatiotemporal distributions of fire spots from open straw burning and

quantifying associated pollutants emissions.

Keywords: Open straw burning; Fire spot; Crop cycle; Greenhouse gas; Emission inventory

Keywords Plus: Open straw burning; MODIS; Fire spot; Accurate extraction; Crop cycle; Crop type; Phenology; Greenhouse gas; Emission inventory; Driving factor; Policy

1 Introduction

Open straw burning, a customary practice in agricultural areas, serves multiple purposes, including rapid straw disposal, weed control, nutrient release, and pest management (Korontzi et al., 2006; Wen et al., 2020). This practice results in short-term yet intense emissions of greenhouse gases (GHGs), such as carbon dioxide (CO_2), methane (CH_4), and nitrous oxide (N_2O). The accumulation of these gases in the atmosphere adversely impacts climate and atmospheric chemistry (Weldemichael and Assefa, 2016; Tang et al., 2020; Hong et al., 2023). To date, open straw burning remains prevalent in grain-producing areas globally, despite the many drawbacks of such a practice (Gadde et al., 2009; Huang et al., 2013; Zhu et al., 2015; Ahmed et al., 2019; Mehmood et al., 2020; Fu et al., 2022; Huang et al.,2023; Xu et al., 2023a). Thus, accurate and high spatial resolution emission inventories for GHGs from this source sector are needed from regional to global scales to assess potential climate and air quality impacts and formulate carbon mitigation policies.

The “bottom-up” approach, which is based on the amount of straw burned and corresponding emission factors, has been widely employed to establish emission inventories for various pollutants emitted from open straw burning (van der Werf et al., 2017; Wang et al., 2018; Liu et al., 2021; Zheng et al., 2023). Emission factors for diverse pollutants released from different types of straw burning have been extensively investigated in laboratory studies (Li et al., 2007; Liu et al., 2011; Stockwell et al., 2014;

Pan et al., 2017; Peng et al., 2016; Sun et al., 2016). However, estimation of the amount of straw burned is subject to large uncertainties since it involves many parameters, such as grain yield, ratio of straw and grain, open burning proportion, burning efficiency, and dry matter fraction (Guan et al., 2017; Zhou et al., 2017). Consequently, existing regional-scale emission inventories based on the "bottom-up" approach generally have large uncertainties and low spatiotemporal resolutions (Tian et al., 2011; Jin et al., 2017).

The advent of satellite technologies, such as Moderate Resolution Imaging Spectroradiometer (MODIS, remote sensing instrument), Visible Infrared Imaging Radiometer Suite (VIIRS, remote sensing instrument), and Himawari-8 (geostationary satellite), has markedly revolutionized the monitoring of open straw burning, enabling real-time and high spatiotemporal resolution fire spot products to be accessible to the general public (Schroeder et al., 2014; Giglio et al., 2016; Xu et al., 2017; Wu et al., 2018; Zhuang et al., 2018; Lv et al., 2024). Many studies have effectively utilized satellite fire spot products for constructing emission inventories, based on either the burned area (BA) or fire spot counts (FC) (Ke et al., 2019; Cui et al., 2021). Several studies have also developed a hybrid inventory strategy using the "bottom-up" approach to allocate GHGs emissions spatially and temporally based on BA or FC (Jin et al., 2018; Zhang et al., 2019; Kumar et al., 2021). These approaches have significantly improved the spatiotemporal resolutions of the emission inventories for open straw burning (Wu et al., 2023).

MODIS and VIIRS, both operating in polar orbits, provide only two observations per day. MODIS has provided 1 km resolution fire data since 2000, which is suitable for long-term trend analyses (Chen et al., 2012); while VIIRS has provided fire data at a 375 m resolution since 2012, which is more suitable for detecting small fires (Chen et al., 2022). Himawari-8 (Geostationary orbit) has provided 10-minute temporal resolution and 2 km spatial resolution fire data since 2015, ideal for real-time monitoring across the Asia-Pacific region (Zhang et al., 2020). However, the aforementioned datasets remain inadequate for accurately capturing small-area, short-duration open straw burning, particularly in scattered farmlands (Wiedinmyer et al., 2014). It should also be noted that meteorological disturbances, such as cloud cover and rainfall, can reduce the accuracy of these products (Schroeder et al., 2014; Ying et al., 2019). Furthermore, straw burning during non-satellite transit periods, on cloudy days, at night, and under heavy haze may not be captured in these datasets (Liu et al., 2020). For example, Liu et al. (2019) found that same-day omission error of MODIS burned area product could be as high as 95% for agricultural fire detection during the post-monsoon season in northwestern India.

With continuous enrichment of satellite data, a strong relationship was observed between fire radiative power (FRP) and emission amounts from open straw burning (Wu et al., 2023). Consequently, the FRP algorithm has been widely accepted for

estimating emissions (Wooster et al., 2005; Freeborn et al., 2008; Vermote et al., 2009; Yang et al., 2019). The FRP algorithm has been optimized by integrating multi-source satellite fire spot data, field survey data, and ground observation data, and combined with advanced modeling techniques to improve the accuracy of emission inventory for open straw burning. For example, Liu et al. (2020) revised FRP by combining household survey results with satellite observations in northern India to capture small fires, fill cloud/haze gaps in satellite observations, and adjust partial-field burns and diurnal cycle of fire activity disturbances. Yang et al. (2020) improved the FRP algorithm by calibrating the contributions of open straw burning to ground observation data in Northeast China based on model simulation results using the coupled Weather Research and Forecasting model and Community Multiscale Air Quality (WRF-CMAQ) model.

At present, the identification of straw types in open straw burning typically relies on crop data, such as the International Geosphere-Biosphere Programme (IGBP)-Modified MODIS Land Use and MapSPAM datasets (Ke et al. 2019; Yang et al. 2020). These low spatiotemporal resolution crop data contribute to errors in both the extraction of fire spots and the identification of straw types (Ke et al., 2019; Liu et al., 2022). Additional errors come from planting structure adjustment and frequent variations in crop phenology. For instance, fire spots occurred during crop growth might be incorrectly classified as open straw burning, while those occurred prior to crop growth

could be inaccurately attributed to burning of straws from subsequent harvests (Zhou et al., 2022). Therefore, high spatiotemporal resolution data on crop types and phenology are critical, and such data should be integrated into the extraction and classification of fire spots from open straw burning to accurately estimate emissions of various pollutants from this source sector.

To control emissions from open straw burning, the "Air Pollution Prevention and Control Action Plan" (APPCAP) took into effect in 2013 in China (Huang et al., 2021). In addition, China committed to achieve carbon peak by 2030 and carbon neutrality by 2060, which draws unprecedented challenges in reducing carbon emissions from open straw burning (Wu et al., 2023). As a significant grain-producing region in China, Northeast China produced 135 million tons of major grains (corn, rice, beans, and wheat) in 2020, accounting for 21.4% of total production in China (National Bureau of Statistics of China, 2021). During 2013-2018, open straw burning in Northeast China exhibited an increasing trend, while decreasing in all other regions of China (Huang et al., 2021). The constant increase reflects the expansion of the agricultural sector and economic development in Northeast China yet relatively unconstrained open burning activities (Huang et al., 2021). Liu et al. (2022) estimated CO_2 emissions from open straw burning in Northeast China to be as high as 344 Tg from 2012 to 2020.

In this study, high spatial resolution fire spot products were used to develop annual

emission inventories of GHGs, including CO_2, CH_4, and N_2O, from open straw burning in Northeast China for the period of 2001-2020. To improve the accuracy of the developed emission inventory, a novel concept that integrates the crop cycle information into fire spot extraction and classification was adopted. Furthermore, this study conducted a thorough analysis to assess the driving factors influencing GHGs emissions during the two decades. This study comprehensively examined GHGs emissions from open straw burning in Northeast China and offered valuable insights to policy makers for mitigating carbon emissions and air pollution in agricultural areas.

2 Methodology

2.1 Extraction and classification of fire spots

The MODIS fire product (MCD14ML, Collection 6.1) was selected from 1 January 2001 to 31 December 2020 for the whole region of Northeast China (Giglio et al., 2016, sftp://fuoco.geog.umd.edu). The dataset, with a spatial resolution of about 1 km^2, includes essential variables, such as latitude, longitude, acquisition date and time (in UTC), satellite (Aqua or Terra), FRP, and fire type (presumably vegetation fire, active volcano, other static land source, and offshore), among others (https://modis-fire.umd.edu/files/MODIS_C6_C6.1_Fire_User_Guide_1.0.pdf). Non-vegetation fire activities (active volcano, other static land source, and offshore) were then filtered out from the selected dataset for subsequent analysis.

To clarify, the MCD14ML underestimated fire spots in 2001 and 2002 because only the Terra satellite was operational before 3 July 2002. Therefore, data for the years of 2003 to 2020 were used for developing annual emission inventories, with relevant results for 2001 and 2002 as reference only. Also, a failure of the Aqua satellite on 16 August 2020 led to the loss of fire spot data for about two weeks (https://modis-fire.umd.edu/files/MODIS_C61_BA_User_Guide_1.1.pdf). However, as August is a crop-growing period in Northeast China, this failure would not lead to an underestimation of fire spots from open straw burning.

The ChinaCropArea1 km and ChinaCropPhen1 km datasets were used to extract and classify fire spots from open straw burning (Luo et al., 2020a; Luo et al., 2020b). These datasets present annual data on the type and phenology (Day of Year (Doy) of emergence and maturity) of grain crops (corn, rice, and wheat). Considering that Northeast China is a major bean-producing area, we also compiled bean distribution datasets (Li et al., 2021; Xuan et al., 2023). However, bean distribution in Jilin and Liaoning provinces was not recorded during 2001-2012 in this dataset. The dataset was extended to the whole region of Northeast China (Heilongjiang, Jilin, and Liaoning provinces) after 2013. Thus, some gaps still exist in these datasets compared to the comprehensive information required for this study, as detailed in **Table S1**.

Fig. 1 describes the meticulous process to accurately extract and classify fire spots from

206 open straw burning in areas experiencing one-harvest season every year. The process
207 involves several key steps:
208 **Step 1)** The current year's ChinaCropPhen1 km and ChinaCropArea1 km, along with
209 the previous year's ChinaCropArea1 km data, were extracted to Fire spots (MCD14ML)
210 by ArcGIS 10.2 software to obtain the Fire spots-Crop-Phen dataset.
211 **Step 2)** Considering the crop cycle, the extraction of fire spots was divided into two
212 stages. The first stage is before crop growth (spring) and requires the fire spot to satisfy
213 two conditions: a) there was a crop planted in the previous year, and b) the burning date
214 is before emergence. The second stage is after crop growth (autumn) and also involves
215 two conditions: a) there was a crop planted in the current year, and b) the burning date
216 is after maturity.
217 **Step 3)** For fire spots in spring, the type of straw burned is identified based on the
218 previous year's crop type. For autumn fire spots, the straw type is determined according
219 to the crop type of the current year.
220
221 Furthermore, fire spots from open straw burning were extracted using the traditional
222 method that does not integrate crop cycle information. Only the current year's
223 ChinaCropArea1 km data was extracted to Fire spots (MCD14ML). Then, fire spots
224 occurring on agricultural land with growing crops were identified as open straw burning.

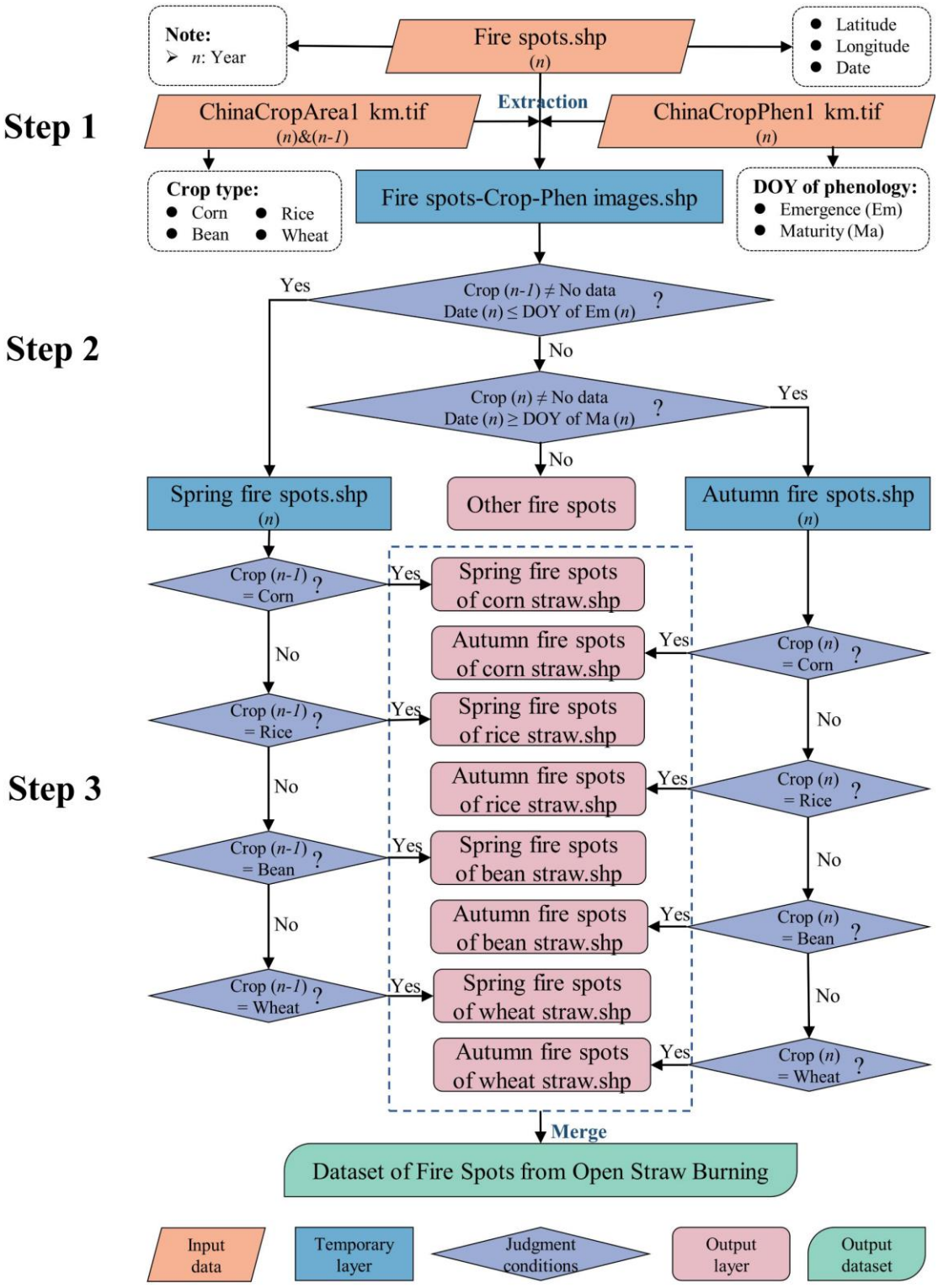

225

226 **Fig. 1** Extraction and classification method for fire spots from open straw burning

2.2 Development of high spatial resolution annual emission inventories for GHGs and exploration of driving factors

Annual emission inventories for GHGs were developed for the region of Northeast China at a grid resolution of 5 km × 5 km for the years of 2001 to 2020. The domain grids were created using Fishnet of ArcGIS 10.2 software.

The modified FRP algorithm (Yang et al., 2020) is used to estimate the emissions of GHGs from open straw burning in this study:

$$E = \alpha \times \int_{t_1}^{t_2} FRP^{*} dt \times \beta \times F = \alpha \times FRP \times f_{FRP} \times (t_2 - t_1) \times \beta \times F \quad (1)$$

where E (in g) is the emissions of GHGs; α is a correction factor used to adjust for *FRP* detection errors between MODIS and VIIRS, which is given a value of 2.5 following Vadrevu and Lasko (2018), indicating that the *FRP* VIIRS sum is 2.5 times of the *FRP* MODIS sum; t_1 and t_2 are the beginning and ending time of fire spots, respectively, and the average burning time (3 hours) of a fire spot in Northeast China was obtained by delivering questionnaires to local farmers (Yang et al., 2020); FRE^{*} (in MW) is adjusted satellite detected *FRP*; *FRP* (in MW) is the instantaneous *FRP* observed by satellite; f_{FRP} is a correction factor that is used to adjust the underestimated emissions by fire spots, and Yang et al. (2020) determined an optimal value of 5 for f_{FRP} by calibrating the contributions of open straw burning to ground observation data in Northeast China using WRF-CMAQ; β (in kg·MJ^{-1}) is biomass combustion rate and the average value of 0.411 kg·MJ^{-1} from previous studies is used here (Wooster et al., 2005; Freeborn et

248 al., 2008); and F (in $g \cdot kg^{-1}$) is the emission factor for individual straw type (**Table 1)**

249 (Li et al., 2007; Liu et al., 2011; Peng et al., 2016).

250

251 **Table 1.** Emission factors of open straw burning for different crop types

Crop	Emission factors ($g \cdot kg^{-1}$)		
	CO_2	CH_4	N_2O
Corn	1350	4.4	0.12
Rice	1460	3.2	0.11
Bean	1445	3.9	0.09
Wheat	1460	3.4	0.05

252

253 Driving factors such as the output of major grains and rural residential coal

254 consumption for temporal variations of annual GHGs emissions were explored through

255 Pearson correlation analysis using SPSS 20.0. Information on the above data is also

256 detailed in **Table S1**.

257 ## 3 Results and discussion

258 ### 3.1 Spatial and temporal distributions of fire spots

259 Cultivated lands in Northeast China primarily distribute in Sanjiang Plain (Northeast

260 Heilongjiang Province), Songnen Plain (West Heilongjiang Province and Midwest Jilin

261 Province), and Liao River Plain (Central Liaoning Province) (**Fig. 2(a)**). Fire spots were

262 widely spread, covering most cultivated lands, including both dry and paddy fields

263 across Northeast China (**Fig. 2(a)** and **2(b)**). A total of 156,044 fire spots from open

264 straw burning were recorded during 2001-2020. Note that the traditional method

265 overestimated the total number of fire sports by 7190 over the 20-year period, with the
266 largest in 2017 (an overestimation of 4060) (**Fig. 2(c)**). This highlights the importance
267 of integrating crop cycle information into fire spot extraction for open straw burning to
268 enhance data accuracy and reliability. Considering the 20-year together (2001-2020),
269 high occurrence frequencies of open straw burning (also referred to as intensity of fire
270 spots below) appeared in the northern Sanjiang Plain, eastern Songnen Plain, and
271 eastern Liao River Plain, as well as scattered areas close to Inner Mongolia (**Fig. 2(a)**
272 and **2(b)**).
273
274 Interannual variations of fire spots distributions are shown in **Fig. S1**. In the Sanjiang
275 Plain, low occurrence frequencies of fire spots were observed in a few cultivated lands
276 during 2003-2006 (**Fig. S1(c)** to **Fig. S1(f)**) and in most cultivated lands in the northern
277 part of the Plain during 2007-2013 (**Fig. S1(g)** to **Fig. S1(m)**). Note that in 2014 and
278 later years, fire spots were extended to the entire Sanjiang Plain, and the northern part
279 of the Plain became an area with high intensity of fire spots (**Fig. S1(n)** to **Fig. S1(q)**),
280 although a few cultivated lands in this Plain recorded low intensity of fire spots after
281 2018 (**Fig. S1(r)** to **Fig. S1(t)**). In the Songnen Plain, most cultivated lands recorded
282 fire spots during 2014 to 2017, with highest intensity in the northern and eastern parts
283 of the Plain (**Fig. S1(n)** to **Fig. S1(q)**). The occurrence frequencies of fire spots
284 decreased across the plain since 2018, particularly in the northern part of the Plain (**Fig.**
285 **S1(r)** to **Fig. S1(t)**). In the Liao River Plain, although fire spots were observed in most

cultivated lands in the eastern part of the Plain during 2014-2017, high occurrence frequency was only recorded in 2014 (**Fig. S1(n)** to **Fig. S1(q)**).

Apparently, open straw burning events decreased in all of the three Plains since 2018 (**Fig. S1(r)** to **Fig. S1(t)**), which was likely due to the intensified effort from the Chinese government banning open straw burning (Hong et al., 2023). The reduction in the number of fire spots was more significant in the Sanjiang Plain and northern Songnen Plain than Liao River Plain (**Fig. S1**), indicating more compliance with straw burning bans from State Farms in the former two regions.

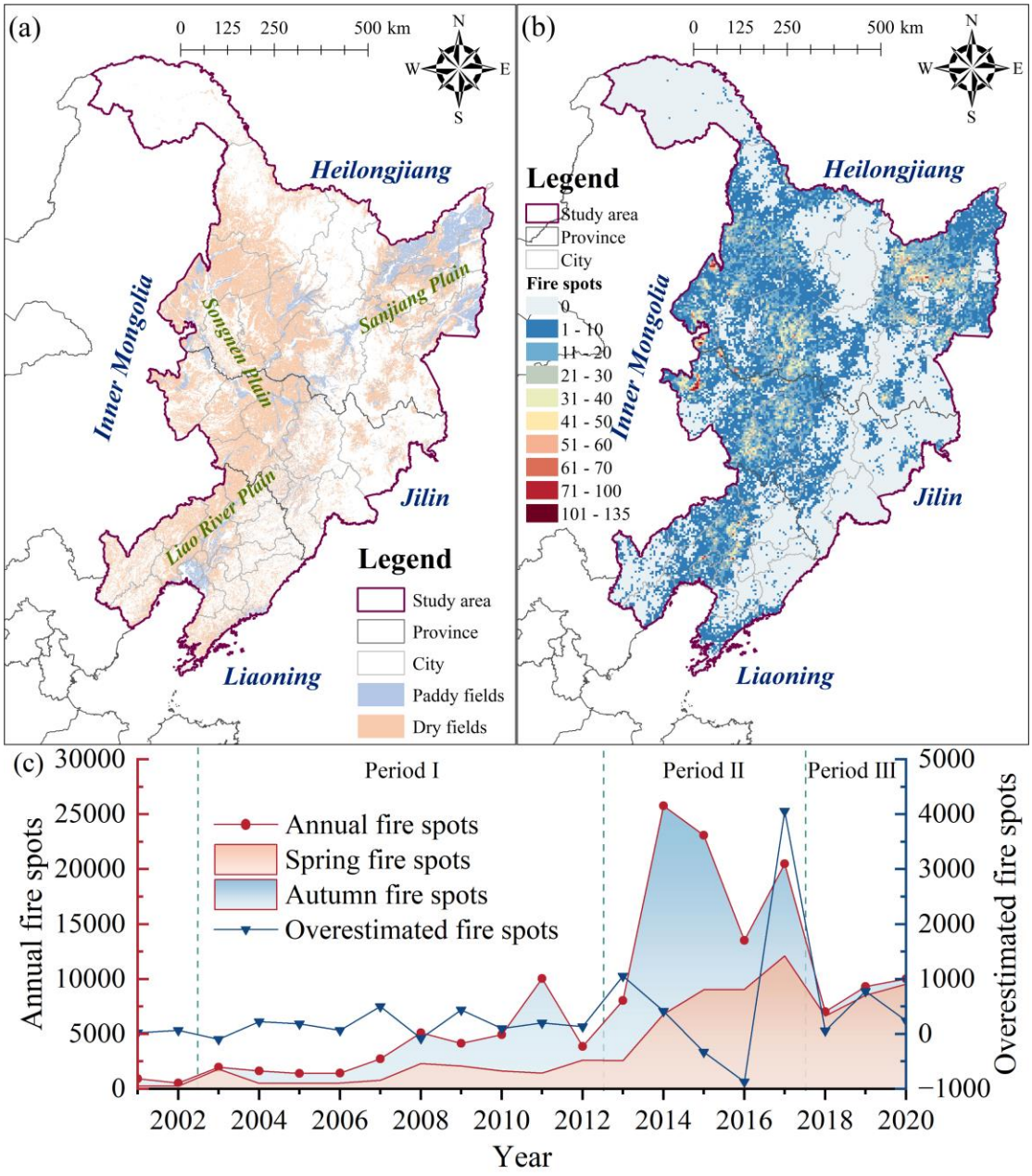

295

296 **Fig. 2** (a) Spatial distributions of cultivated land in 2020 in Northeast China
297 (https://www.resdc.cn), (b) spatial distributions of the total number of fire spots during 2001-
298 2020 in Northeast China, and (c) seasonal distributions of the annual fire spots, and annual
299 overestimated fire spots by the traditional method from 2001 to 2020. The overestimated fire
300 spots are calculated as the number of fire spots identified by the traditional method minus those
301 extracted by the novel method.

Fire spots from open straw burning concentrated in spring and autumn, with few burning events in the other two seasons in Northeast China. Open straw burning events in this region during 2003-2020 can be roughly divided into three distinctive periods (**Fig. 2(c)**). During **Period I** (2003-2012), the annual average number of fire spots in this region was 3732. There were more fire spots in autumn than spring in most of these years. During **Period II** (2013-2017), there was a substantial surge in fire spots, with an annual average of 18,177 spots, accounting for 58.2% of the 20-year total. Notably, the number of fire spots peaked at 25,759 in 2014. Spring fire spots consistently increased annually, reaching the highest in 2017 at 12,094 spots. The variations for autumn fire spots were fluctuating, with a peak of 18,951 spots in 2014. During 2013-2015, autumn fire spots were higher than spring; however, this trend reversed in 2016 and 2017, with spring fire spots becoming more dominant. During **Period III** (2018-2020), the number of fire spots experienced a significant decrease, averaging 8,788 spots annually, which was a 51.7% decrease from **Period II**. Spring emerged as the primary season of fire spots, accounting for approximately 93.8% of the annual total. Zhao et al. (2021) have reported a similar phenomenon, in which the primary season of open straw burning in Northeast China gradually shifts to spring (April to June). The apparent seasonal variations of open straw burning primarily stems from strict government bans imposed after the autumn harvest (Yang et al., 2020). In addition, farmers' increasing awareness regarding how open straw burning contributes

to the thawing of spring soil may also be a factor (Saxton et al., 1993; Song et al., 2024).

However, the "sudden drop" in fire spots should also be partially attributed to strategies employed by farmers to avoid detection by satellite and government regulations, such as burning straw on smaller scales and in more dispersed areas, or during non-transit times of the satellites (Liu et al. 2019; Liu et al. 2020). Chen et al. (2022) also found that farmers in East China frequently burned straw in 2019 during non-transit times of MODIS/VIIRS satellites, as indicated by Himawari satellite data. To further verify the reliability of the "sudden drop" in fire spots in Northeast China, we analyzed the trend of particulate matter concentrations (PM_{10} and $PM_{2.5}$) during the periods of open straw burning from 2014 to 2020 in Northeast China (**Fig. S2**). Atmospheric particulate matter concentrations during autumn open straw burning in Northeast China decreased with a "sudden drop" in fire spots (**Fig. S2(c)**). However, a similar trend was not observed in spring (**Fig. S2(b)**), possibly due to limitations in fire spot detection by current satellite techniques and avoidance strategies. Kumar et al. (2021) suggested that a hybrid inventory, which accurately allocates emissions estimated using the "bottom-up" approach based on satellite data, may be more advantageous in this scenario.

The straw burning dates in Northeast China also changed during the three periods, besides varying with crop type. During **Period I** (2003-2012), the autumn burning dates of corn and rice straws were concentrated from early October to mid-November (DOY

range of 270 to 320). Spring burning dates of corn and rice straw were concentrated between mid-March and late April (DOY range of 70 to 120) in 2003, while dispersed to early March to mid-May (DOY range of 60 to 140) in 2012 (**Fig. 3(a)** and **Fig. 3(b)**). During **Period II** (2013-2017), the dispersion of spring burning dates for corn and rice straws became more pronounced, extending from early February to mid-May (DOY range of 30 to 140) **(Fig. 3(a)** and **Fig. 3(b)**). During **Period III** (2018-2020), the dispersion of spring burning dates for corn and rice straws persisted (**Fig. 3(a)** and **Fig. 3(b)**). During **Period I** (2003-2012), the spring and autumn burning dates of bean straw in Heilongjiang Province were concentrated from mid-March to late April (DOY range of 70 to 120) and from early October to mid-November (DOY range of 270 to 320), respectively (**Fig. 3(c)**). During 2013-2020, the spring burning dates of bean straw in Northeast China were concentrated between early February and late April (DOY range of 30 to 120), while the autumn burning dates remained consistent with those during **Period I** in Heilongjiang Province (**Fig. 3(c)**). Unlike other crops, the burning dates for wheat straw did not conform to the aforementioned pattern of variation, likely due to a limited number of fire spots (**Fig. 3(d)**). The changing dispersion of burning dates for each crop type indicates shifts in agricultural practices that may be influenced by regional straw burning ban policies, environmental conditions, and farming practices (Yang et al., 2020).

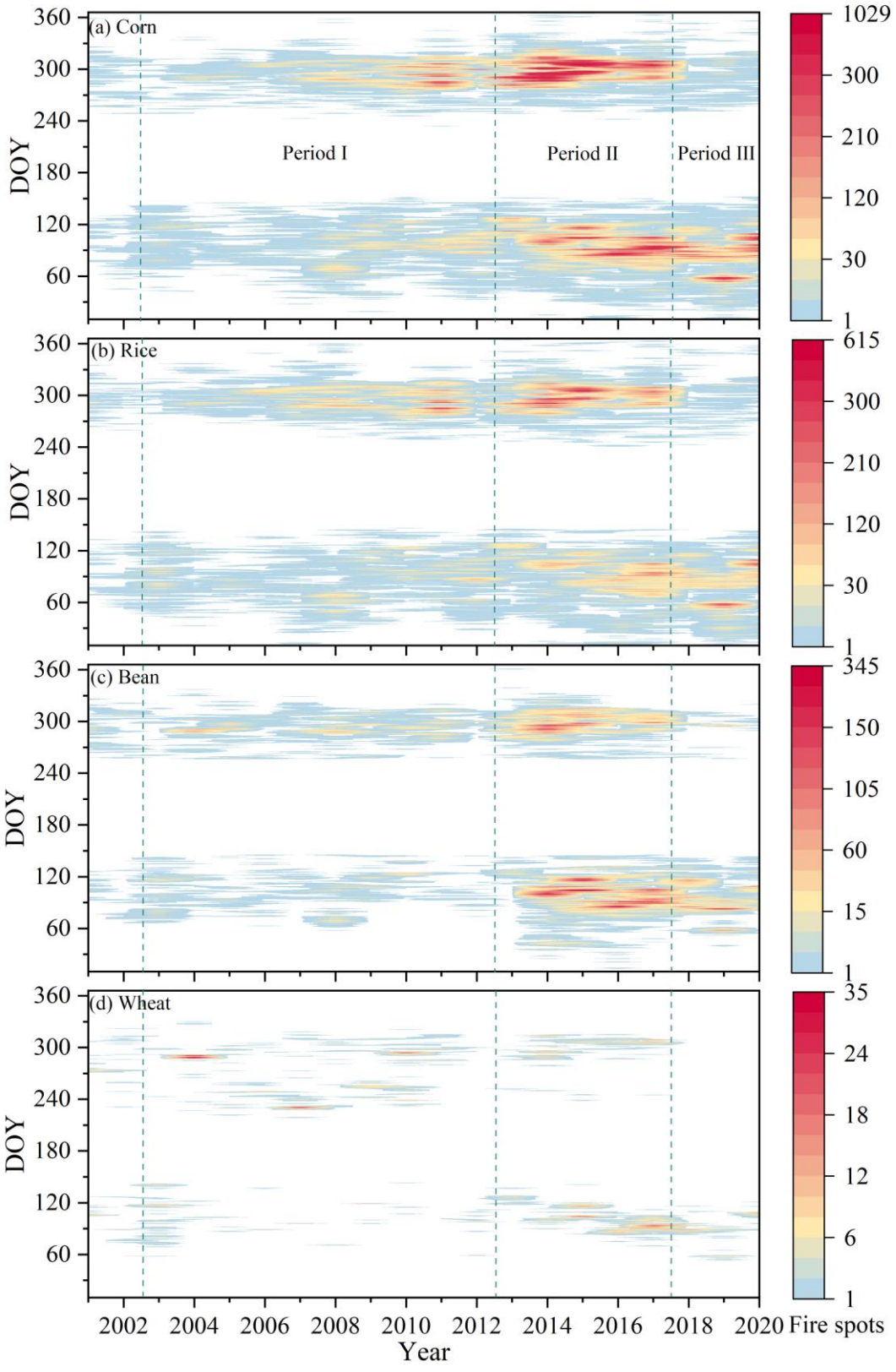

Fig. 3 The daily frequency distribution of fire spots from various straws burning: (a), (b), (c), and (d) represent corn, rice, bean, and wheat straw, respectively. Note: The x-axis is Year; the

y-axis is DOY; and the range of colorbars (indicating fire spots) is different for each crop, with values ranging from 1 to 1,029 for corn, 1 to 615 for rice, 1 to 345 for beans, and 1 to 35 for wheat.

3.2 High spatial resolution annual emission inventory of GHGs

The cumulative emissions of CO_2, CH_4, and N_2O from open straw burning in Northeast China from 2001 to 2020 amounted to 198 Tg, 557 Gg, and 15.7 Gg, respectively (or 218 Tg CO_2-eq in total). The spatial distributions of GHGs emissions correspond well with those of fire spots, particularly in high emission areas (**Fig. 2** and **Fig. 4**). However, the amounts of GHGs emissions in the northern Songnen Plain unexpectedly exceeded those in the eastern Songnen Plain and eastern Liao River Plain, suggesting that even low intensity fire spots can generate considerable emissions of GHGs due to higher FRP detected via remote sensing. Therefore, the FRP algorithm proves to be more effective than burned areas-based algorithms in identifying emission intensity resulted from open straw burning while reducing the uncertainty associated with high spatiotemporal resolution emission inventory (Wu et al., 2023).

The annual emissions of CO_2, CH_4, N_2O, and CO_2-eq from 2001 to 2020 are presented in **Figs**. **S3**, **S4**, **S5**, and **S6**, respectively. The spatiotemporal patterns of GHGs emissions correspond well to the observed trends in fire spots during **Period I** (2003-2012). However, during **Period II** (2013-2017) and **Period III** (2018-2020), the emissions of GHGs in the eastern Songnen Plain and eastern Liao River Plain did not

exhibit a proportional increase with the rise in fire spots. This discrepancy can be attributed to the dispersed burning dates among individual farmers in these regions, resulting in high intensity fire spots with relatively low emissions. In contrast, several State Farms located in the northern Sanjiang Plain and northern Songnen Plain demonstrated a higher level of synchronization in open straw burning activities, resulting in parallel trends between fire spots and emissions (Cui et al., 2021).

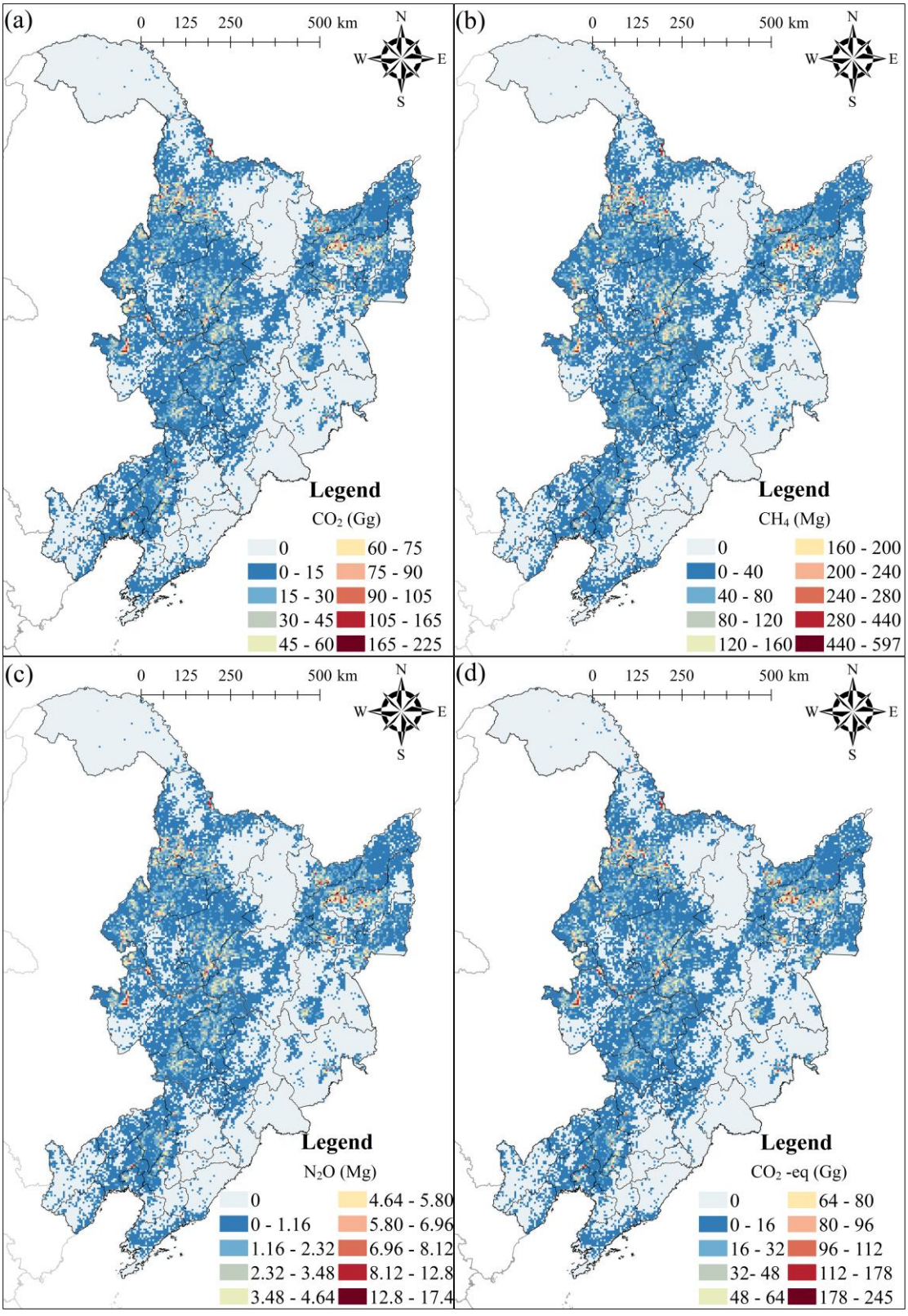

Fig. 4 The cumulative GHGs emissions from open straw burning in Northeast China from 2001 to 2020 for CO_2 (a), CH_4 (b), N_2O (c), and CO_2-eq (d) emissions, respectively. Note: The range of colorbars (indicating emissions) is different for each GHG, with values ranging from 0 to

225 Gg for CO_2, 0 to 597 Mg for CH_4, 0 to 17.4 Mg for N_2O, and 0 to 245 Gg for CO_2-eq.

During **Period I** (2003 - 2012), average annual CO_2-eq emission was at 4.20 Tg, and the cumulative CO_2-eq emission amounted to 42.0 Tg. During **Period II** (2013 - 2017), average annual CO_2-eq emission increased substantially to 26.1 Tg, and the cumulative emission during this period amounted to 130 Tg, which accounted for 59.9% of the total emissions over the two decades. During **Period III** (2018 - 2020), average annual CO_2-eq emissions decreased significantly to 14.3 Tg, and the cumulative emission during this period amounted to 42.8 Tg (**Fig. 5(a)**). The trend of CO_2-eq emission from 2003 to 2020 generally corresponds with the occurrence of fire spots, except for 2015 when higher emissions were obtained despite having fewer fire spots than the case in 2014 (**Fig. 5(a)**). Such a trend is consistent with those of carbonaceous gases and aerosols (CGA) emissions estimated by Liu et al., (2022). This discrepancy between fire spots and pollutant emissions in 2015 highlights the limitations of estimating pollutant emissions based solely on burned areas (Ke et al., 2019; Wu et al. 2023). The combustion of corn and rice straw was identified as the primary contributors to CO_2-eq emissions, accounting for 51.1% and 30.8%, respectively, of the total emissions (**Fig. 5(b)**). Specifically, corn straw burning released 99.6, 9.06, and 2.42 Tg, while rice straw burning released 61.8, 3.78, and 1.27 Tg of CO_2, CO_2-eq for CH_4, and CO_2-eq for N_2O, respectively.

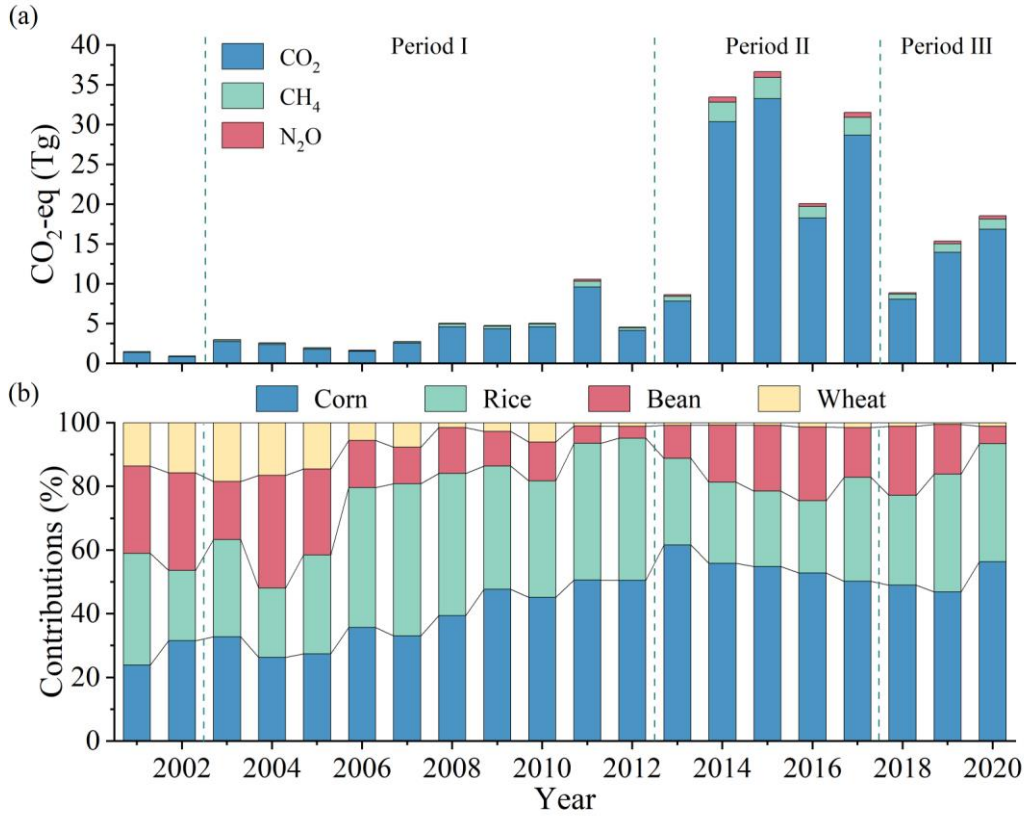

418

419 **Fig. 5** (a) Regional total annual CO_2-eq emissions and (b) percentage contributions from open

420 burning of individual crop straw type.

421 **3.3 Validation and limitations**

422 Our estimated total CO_2 emissions from 2012 to 2020 with MODIS (161 Tg) or with

423 VIIRS (165 Tg) were much lower than that (~ 523 Tg) estimated by Liu et al. (2022),

424 the latter was based on a modified FRP algorithm and fire spot products by VIIRS,

425 which has limitations in its traditional straw extraction methods in accurately

426 identifying fire spots during certain times of the year. Our estimated CO_2 emission from

427 2002 to 2020 in Northeast China (196 Tg) was slightly lower than that (195 Tg)

428 estimated by Global Fire Emissions Database Version 4.1 (GFED4.1s) by van der Werf et al.

429 (2017), and slightly higher than that (181 Tg) estimated from the Fire Inventory from

NCAR version 2.5 (FINNv2.5) by Wiedinmyer et al. (2023), which addresses the underestimation of open biomass burning in China by the older version FINNv1.5 (Stavrakou et al., 2016; Yang et al., 2020) (**Fig. 6**). However, our estimated total CO_2 emission from 2012 to 2020 was significantly higher than that (35.6 Tg) estimated by VIIRS-based Fire Emission Inventory version 0 (VFEIv0) by Ferrada et al. (2022), which relies on the traditional FRP algorithm (**Fig. 6**). Furthermore, Northeast China surpassed East China (27.1 Tg) as the highest emitter from open straw burning in China since 2014, with CO_2 emissions reaching 30.4 Tg (Zhang et al. 2020).

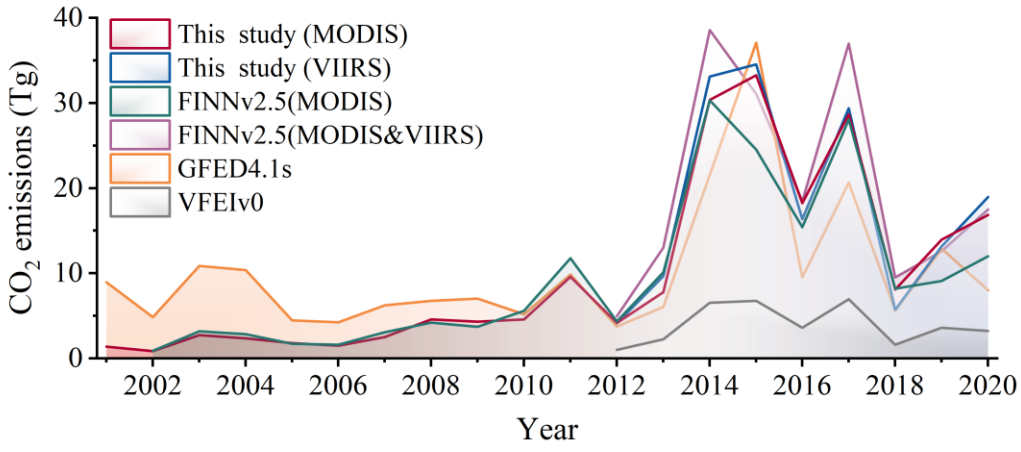

Fig. 6 Annual total emissions of CO_2 from open straw burning (agricultural waste burning) in Northeast China from this study with MODIS (red, 2001-2020) and VIIRS (blue, 2012-2020), the Fire Inventory from NCAR version 2.5 (FINNv2.5) with MODIS-only (green, 2002-2020), FINNv2.5 with MODIS and VIIRS (purple, 2012-2020), Global Fire Emissions Database Version 4.1 (GFED4.1s) (orange, 2001-2020), and VIIRS-based Fire Emission Inventory version 0 (VFEIv0) (grey, 2012-2020).

Although this study effectively improved the accuracy of emission inventory for open

straw burning through the novel method that integrates crop cycle information into extraction and classification of fire spots and the modified FRP algorithm, certain limitations still exist. The uncertainty in this study stems mainly from the inherent limitations of satellite fire detection systems. The MODIS fire spot product, although widely used, is limited by its temporal resolution and tends to miss transient or small-scale fires. In addition, straw burning during non-satellite transit periods, on cloudy days, at night, and under heavy haze further exacerbates the underestimation of fire incidence, leading to potential gaps in emission inventories.

Additionally, the novel method that integrates crop cycle information into extraction and classification of fire spots presents a promising advancement. However, its applicability is constrained to regions where comprehensive and detailed crop data are available. In countries or regions lacking such agricultural information, this method may face challenges, thereby limiting its broader applicability. These factors underscore the need for continued refinement of satellite detection technologies and the expansion of agricultural data collection efforts to reduce uncertainties and enhance the robustness of emission inventories on regional to global scales.

3.4 Driving factors of open straw burning

Open straw burning is more prominently influenced by anthropogenic activities compared to other types of open biomass burning, such as forest, shrubland, and grassland fires (Syphard et al., 2017; Wu et al., 2020). Open straw burning is influenced

by changes in straw yield and utilization rate, straw burning ban policy, and farmers' awareness of straw burning consequences (Chen et al., 2016; Li et al., 2017; Tao et al., 2018; Fang et al., 2019; Xu et al., 2023b).

Northeast China has experienced a remarkable expansion in its sown area for major grain crops over the past two decades. By 2020, the sown area reached 231,937 km^2, 61.4% more than that in 2001 (National Bureau of Statistics of China, 2002-2021). In the meantime, annual straw yield reached 143 Tg in 2020, 142% higher than that (59.2 Tg) in 2001 (**Fig.7**) (numbers are calculated based on the major grain yields in Northeast China presented in National Bureau of Statistics of China (2002-2021) and the ratio of straw and grain (Wang et al.,2012)). Note that the annual straw yields have stabilized around 140 Tg since 2017, and this trend is expected to persist for many years to come (**Fig. 7**). From 2003 to 2020, a strong positive correlation was observed between the straw yields and the emissions of CO_2-eq from open straw burning across Northeast China, as well as in Heilongjiang and Jilin provinces ($p < 0.01$, **Table S2**). If looking at individual periods, significant correlations were only observed during **Period I** (2003-2012) for the whole of Northeast China ($p < 0.01$) and Heilongjiang ($p < 0.01$) (**Table S2**). This highlights that increased straw yields exacerbated the challenges of straw disposal in Northeast China and have been a major contributor to the increase in the emissions of GHGs from open straw burning in the aforementioned region and period.

Besides open burning, crop straw is also used for cooking and heating in rural households in Northeast China (Ke et al., 2023; Liu et al., 2023). Crop straw can also be converted to bioenergy, used as animal feed, and returned to the fields (Alengebawy et al., 2022; Fang et al., 2022). However, exact quantification of straw utilization in different sectors in Northeast China is still lacking (Shi et al., 2023). Knowing that coal combustion and straw burning are major energy sources for rural households in Northeast China, we tried to explore potential changes in straw utilization on open straw burning through coal consumption changes (Fang et al. 2019). The abrupt increase in rural residential coal consumption in 2013 in Northeast China coincided with a spike in CO_2-eq emissions from open straw burning (**Fig. 7(a)**). Furthermore, a significant positive correlation between rural residential coal consumption and CO_2-eq emissions in Northeast China was revealed, especially in Heilongjiang and Jilin provinces (**Table S3**). We thus speculate that the increase in rural commercial energy consumption may have reduced the demand for straw as an energy source for agricultural households, thus facilitating the increased open straw burning. This needs to be confirmed in future studies once various straw utilization pathways are quantified.

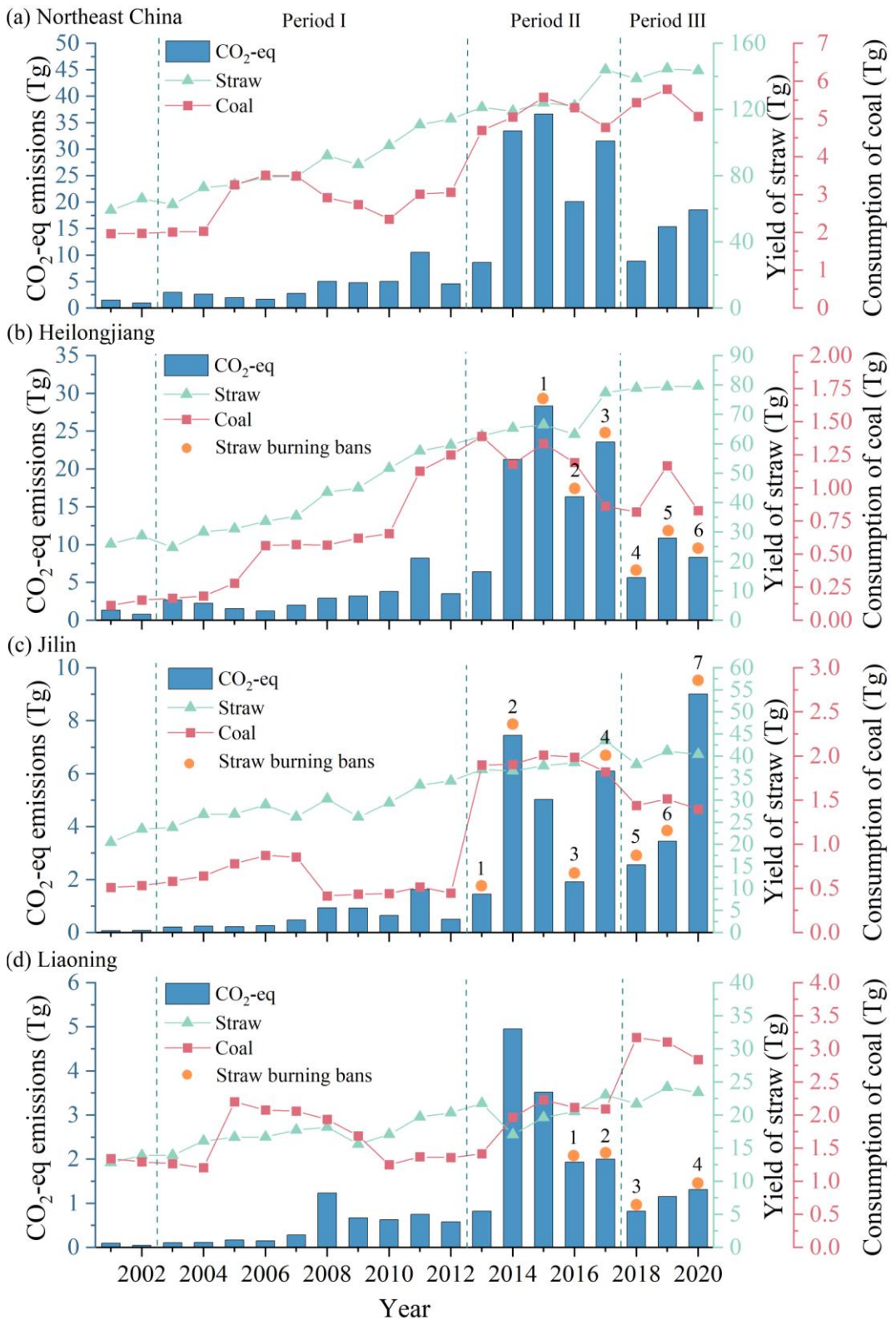

506

507 **Fig. 7** Annual CO_2-eq emissions, yield of straw, rural residential coal consumption, and straw

508 burning bans in (a) Northeast China, (b) Heilongjiang, (c) Jilin, and (d) Liaoning from 2001 to

509 2020. Note: The range of y-axis is different for each region. The blue y-axis indicates CO_2-eq

emissions, with values ranging from 0 to 50 Tg for Northeast China, 0 to 35 Tg for Heilongjiang, 0 to 10 Tg for Jilin, and 0 to 6 Tg for Liaoning; the green y-axis indicates yield of straw, with values ranging from 0 to 160 Tg for Northeast China, 0 to 90 Tg for Heilongjiang, 0 to 60 Tg for Jilin, and 0 to 40 Tg for Liaoning; and the red y-axis indicates rural residential coal consumption, with values ranging from 0 to 7 Tg for Northeast China, 0 to 2 Tg for Heilongjiang, 0 to 3 Tg for Jilin, and 0 to 4 Tg for Liaoning.

We also evaluated the efficacy of straw burning ban policy in Heilongjiang, Jinlin, and Liaoning (**Table S4**). Despite the implementation of the policy since 2013 in this region, a significant reduction in CO_2-eq emissions from open straw burning was only observed after 2018 (**Fig. 7**). Compared to the other regions of China, the effective control of open straw burning was delayed by several years in Northeast China (Huang et al., 2021). An important phenomenon was observed regarding the geographical and temporal expansion of the ban policy, e.g., initially focused on key areas and specific seasons (autumn and winter) and progressively extended to the entire region and throughout the whole year (see Heilongjiang Province as an example, **Table S4**). Therefore, enhanced enforcement of the ban policy likely reduced CO_2-eq emissions during **Period III** and shifted the burning season to spring.

In conclusion, the enforcement of region-specific straw burning bans tailored to spatiotemporal variations is crucial to control GHGs emissions, given the anticipated

sustained high straw yields in the future. Additionally, promoting diverse methods for utilizing straw is highlighted as an effective strategy for mitigating carbon emissions resulted from open straw burning in Northeast China. A combined effort on policy enforcement and alternative straw usage would play a pivotal role in addressing the environmental challenges posed by agricultural practices in the region.

4 Conclusions

This study provides a comprehensive analysis of the spatiotemporal variations of open straw burning across Northeast China from 2001 to 2020 and develops regional scale high spatial resolution annual emission inventories of GHGs. Open straw burning in Northeast China emitted a total of 218 Tg of CO_2-eq during 2001-2020, of which 19.3% was from **Period I** (2003-2012), 59.9% from **Period II** (2013-2017), and 19.7% from **Period III** (2018-2020). Analysis results demonstrate the necessity of integrating the crop cycle information into the extraction and classification of fire spots from open straw burning to enhance the accuracy of emission inventories of various pollutants. This study also highlights the inconsistencies between the number of fire spots and pollutant emissions caused by remote sensing detection techniques. In Northeast China, regions such as the northern Sanjiang Plain, eastern and northern Songnen Plain, and eastern Liao River Plain are identified as high-emission areas of GHGs from open straw burning, which emitted 38.1, 45.5, 31.9, and 10.8 Tg of CO_2-eq, respectively, during

2001-2020. Additionally, it is observed that the season for open straw burning has shifted from autumn to spring, with dispersed burning dates. This spatiotemporal analysis provides crucial insights into policy effectiveness as well as geographical variations regarding compliance with regulations banning open straw burning. Consequently, government policies prohibiting open straw burning should be adjusted according to the observed spatiotemporal variations in different regions. Simultaneously promoting diversified applications of straw, such as bioenergy conversion, animal feeding, and soil amendment, is recommended — a strategy that is aligned with China's dual-carbon objectives aiming at achieving carbon peak and carbon neutrality.

Competing interests

At least one of the (co-)authors is a member of the editorial board of Atmospheric Chemistry and Physics.

Acknowledgments

This work was supported by the Distinguished Youth Science Foundation of Heilongjiang Province (JQ2023E001) and Young Leading Talents of Northeast Agricultural University (NEAU2023QNLJ-013).

570

571 **References**

572 Ahmed, W., Tan, Q., Ali, S., and Ahmad, N.: Addressing environmental implications of
573 crop stubble burning in Pakistan: innovation platforms as an alternative approach, Int.
574 J. Global Warming, 19, 76-93, https://doi.org/10.1504/IJGW.2019.101773, 2019.
575 Alengebawy, A., Mohamed, B.A., Ran, Y., Yang, Y., Pezzuolo, A., Samer, M., and Ai,
576 P.: A comparative environmental life cycle assessment of rice straw-based bioenergy
577 projects in China, Environ. Res., 212, 113404,
578 https://doi.org/10.1016/j.envres.2022.113404, 2022.
579 Chen, J.X., Li, R., Tao, M.H., Wang, L.L., Lin, C.Q., Wang, J., Wang, L.C., Wang, Y.,
580 Chen, L.F.: Overview of the performance of satellite fire products in China:
581 Uncertainties and challenges, Atmos. Environ., 268, 118838,
582 https://doi.org/10.1016/j.atmosenv.2021.118838, 2022.
583 Chen, Y.L., Shen, H.Z., Zhong, Q.R., Chen, H., Huang, T.B., Liu, J.F., Cheng, H.F.,
584 Zeng, E.Y., Smith, K.R., and Tao, S.: Transition of household cookfuels in China from
585 2010 to 2012, Appl. Energ., 184, 800-809,
586 https://doi.org/10.1016/j.apenergy.2016.07.136, 2016.
587 Cui, S., Song, Z.H., Zhang, L.M., Shen, Z.X., Hough, R., Zhang, Z.L., An, L.H., Fu,
588 Q., Zhao, Y.C., and Jia, Z.Y.: Spatial and temporal variations of open straw burning
589 based on fire spots in northeast China from 2013 to 2017, Atmos. Environ., 244, 117962,

https://doi.org/10.1016/j.atmosenv.2020.117962, 2021.

Fang, Y.R., Wu, Y., and Xie, G.H.: Crop residue utilizations and potential for bioethanol production in China, Renew. Sust. Energ. Rev., 113, 109288, https://doi.org/10.1016/j.rser.2019.109288, 2019.

Fang, Y.R., Zhang, S.L., Zhou, Z.Q., Shi, W.J., and Xie, G.H.: Sustainable development in China: Valuation of bioenergy potential and CO_2 reduction from crop straw, Appl. Energ., 322, 119439, https://doi.org/10.1016/j.apenergy.2022.119439, 2022.

Ferrada, G.A., Zhou, M., Wang, Jun., Lyapustin, A., Wang, Y.J., Freitas, S.R., and Carmichael, G.R.: Introducing the VIIRS-based Fire Emission Inventory version 0 (VFEIv0), Geosci. Model Dev., 15, 8085-8109, https://doi.org/10.5194/gmd-15-8085-2022, 2022.

Freeborn, P.H., Wooster, M.J., Hao, W.M., Ryan, C.A., Nordgren, B.L., Baker, S.P., and Ichoku, C.: Relationships between energy release, fuel mass loss, and trace gas and aerosol emissions during laboratory biomass fires, J. Geophys. Res-Atmos., 113, D01301, https://doi.org/10.1029/2007JD008679, 2008.

Fu, J., Song, S.T., Guo, L., Chen, W.W., Wang, P., Duanmu, L.J., Shang, Y.J., Shi, B.W., and He, L.Y.: Interprovincial joint prevention and control of open straw burning in Northeast China: Implications for atmospheric environment management, Remote Sens., 14(11), 2528, https://doi.org/10.3390/rs14112528, 2022.

Gadde, B., Bonnet, S., Menke, C., and Garivait, S.: Air pollutant emissions from rice straw open field burning in India, Thailand and the Philippines, Environ. Pollut., 157,

611 1554-1558, https://doi.org/10.1016/j.envpol.2009.01.004, 2009.
612 Giglio, L., Schroeder, W., and Justice, C.O.: The collection 6 MODIS active fire
613 detection algorithm and fire products, Remote Sens. Environ., 178, 31-41,
614 https://doi.org/10.1016/j.rse.2016.02.054, 2016.
615 Guan, Y.N., Chen, G.Y., Cheng, Z.J., Yan, B.B., and Hou, L.A.: Air pollutant emissions
616 from straw open burning: A case study in Tianjin, Atmos. Environ., 171, 155-164,
617 https://dx.doi.org/10.1016/j.atmosenv.2017.10.020, 2017.
618 Hong, X., Zhang, C., Tian, Y., Wu, H., Zhu, Y., and Liu, C.: Quantification and
619 evaluation of atmospheric emissions from crop residue burning constrained by satellite
620 observations in China during 2016-2020, Sci. Total. Environ., 865, 161237,
621 https://doi.org/10.1016/j.scitotenv.2022.161237, 2023.
622 https://modis-fire.umd.edu/files/MODIS_C61_BA_User_Guide_1.1.pdf
623 https://modis-fire.umd.edu/files/MODIS_C6_C6.1_Fire_User_Guide_1.0.pdf
624 Huang, K., Zhuang, G., Lin, Y., Wang, Q., Fu, J.S., Fu, Q., Liu, T., and Deng, C.: How
625 to improve the air quality over megacities in China: pollution characterization and
626 source analysis in Shanghai before, during, and after the 2010 World Expo, Atmos.
627 Chem. Phys., 13, 5927-5942, https://doi.org/10.5194/acp-13-5927-2013, 2013.
628 Huang, L., Zhu, Y.H., Liu, H.Q., Wang, Y.J., Allen, D.T., Ooi, M.C.G.,
629 Manomaiphiboon, K., Latif, M.T., Chan, A., and Li, L.: Assessing the contribution of
630 open crop straw burning to ground-level ozone and associated health impacts in China
631 and the effectiveness of straw burning bans, Environ. Int., 171, 107710,

https://doi.org/10.1016/j.envint.2022.107710, 2023.

Huang, L., Zhu, Y.H., Wang, Q., Zhu, A.S., Liu, Z.Y., Wang, Y.J., Allen, D.T., and Li, L.: Assessment of the effects of straw burning bans in China: Emissions, air quality, and health impacts, Sci. Total Environ., 789, 147935, https://doi.org/10.1016/j.scitotenv.2021.147935, 2021.

Huang, X., Li, M.M., Li, J.F., and Song, Y.: A high-resolution emission inventory of crop burning in fields in China based on MODIS Thermal Anomalies/Fire products, Atmos. Environ., 50, 9-15, https://doi.org/10.1016/j.atmosenv.2012.01.017, 2012.

Jin, Q., Ma, X., Wang, W., Yang, S., and Guo, F.: Temporal and spatial variations of $PM_{2.5}$ emissions from crop straw burning in eastern China during 2000-2014. Acta Sci. Circumstantiae, 37, 460-468, 2017. (in Chinese)

Jin, Q.F., Ma, X.Q., Wang, G.Y., Yang, X.J., and Guo, F.T.: Dynamics of major air pollutants from crop residue burning in mainland China, 2000-2014, J. Environ. Sci., 70, 190-205, https://doi.org/10.1016/j.jes.2017.11.024, 2018.

Ke, H.B., Gong, S.L., He, J.J., Zhou, C.H., Zhang, L., and Zhou, Y.K.: Spatial and temporal distribution of open bio-mass burning in China from 2013 to 2017, Atmos. Environ., 210, 156-165, https://doi.org/10.1016/j.atmosenv.2019.04.039, 2019.

Ke, Y.X., Zhang, F.X., Zhang, Z.L., Hough, R., Fu, Q., Li, Y.F., and Cui, S.: Effect of combined aging treatment on biochar adsorption and speciation distribution for Cd (II), Sci. Total Environ., 867, 161593, http://doi.org/10.1016/j.scitotenv.2023.161593, 2023.

Korontzi, S., McCarty, J., Loboda, T., Kumar, S., and Justice, C.: Global distribution of

653 agricultural fires in croplands from 3 years of Moderate Resolution Imaging
654 Spectroradiometer (MODIS) data, Global Biogeochem. Cy., 20, GB2021,
655 https://doi.org/10.1029/2005GB002529, 2006.
656 Kumar, A., Hakkim, H., Sinha, B., and Sinha, V.: Gridded 1 km × 1 km emission
657 inventory for paddy stubble burning emissions over north-west India constrained by
658 measured emission factors of 77 VOCs and district-wise crop yield data, Sci. Total
659 Environ., 789, 48064, https://doi.org/10.1016/j.scitotenv.2021.
660 148064, 2021.
661 Li, C.L., Hu, Y.J., Zhang, F., Chen, J.M., Ma, Z., Ye, X.N., Yang, X., Wang, L., Tang,
662 X.F., Zhang, R.H., Mu, M., Wang, G.H., Kan, H.D., Wang, X.M., and Mellouki, A.:
663 Multi-pollutant emissions from the burning of major agricultural residues in China and
664 the related health-economic effects, Atmos. Chem. Phys., 17, 4957-4988,
665 https://doi.org/10.5194/acp-17-4957-2017, 2017.
666 Li, X.H., Wang, S.X., Duan, L., Hao, J.M., Li, C., Chen, Y.S., and Yang, L.: Particulate
667 and trace gas emissions from open burning of wheat straw and corn stover in China,
668 Environ. Sci. Technol., 41(17), 6052-6058, https://doi.org/10.1021/es0705137, 2007.
669 Li, X.Y., Yu, L., Peng, D.L., and Gong, P.: A large-scale, long time-series (1984-2020)
670 of soybean mapping with phenological features: Heilongjiang Province as a test case,
671 Int. J. Remote Sens., 42, 7332-7356, https://doi.org/10.1080/01431161.2021.1957177,
672 2021.
673 Liu, L.H., Jiang, J.Y., and Zong, L.G.: Emission inventory of greenhouse gases from

674 agricultural residues combustion: A case study of Jiangsu Province, Environ. Sci., 32,
675 1242-1248, 2011. (In Chinese)
676 Liu, T.J., Marlier, M.E., Karambelas, A., Jain, M., Singh, S., Singh, M.K., Gautam, R.,
677 DeFries, R.S.: Missing emissions from post-monsoon agricultural fires in northwestern
678 India: regional limitations of MODIS burned area and active fire products, Environ.
679 Res. Commun., 1, 011007, https://doi.org/10.1088/2515-7620/ab056c, 2019.
680 Liu, T.J., Mickley, L.J., Singh, S., Jain, M., DeFries, R.S., Marlier, M.E.: Crop residue
681 burning practices across north India inferred from household survey data: Bridging
682 gaps in satellite observations, Atmos. Environ. - X, 8, 100091,
683 https://doi.org/*11883*10.1016/j.aeaoa.2020.100091, 2020.
684 Liu, Y.X., Zhao, H.M., Zhao, G.Y., Zhang, X.L., and Xiu, A.J.: Carbonaceous gas and
685 aerosol emissions from biomass burning in China from 2012 to 2021, J. Clean. Prod.,
686 362, 132199, https://doi.org/10.1016/j.jclepro.2022.132199, 2022.
687 Liu, Y.Z., Zhang, J., and Zhuang, M.H.: Bottom-up re-estimations of greenhouse gas
688 and atmospheric pollutants derived from straw burning of three cereal crops production
689 in China based on a national questionnaire, Environ. Sci. Pollut. Res., 28, 65410-65415,
690 https://doi.org/10.1007/s11356-021-15658-9, 2021.
691 Liu, Z.K., Cui, S., Fu, Q., Zhang, F.X., Zhang, Z.L., Hough, R., An, L.H., Li, Y.F., and
692 Zhang, L.M.: Transport of neonicotinoid insecticides in a wetland ecosystem: has the
693 cultivation of different crops become the major sources? J. Environ. Manag. 339,
694 117838, https://doi.org/10.1016/j.scitotenv.2023.161593, 2023.

Luo, Y.C., Zhang, Z., Li, Z.Y., Chen, Y., Zhang, L.L., Cao, J., and Tao, F.L.: Identifying the spatiotemporal changes of annual harvesting areas for three staple crops in China by integrating multi-data sources. Environ. Res. Lett., 15, 074003, https://doi.org/10.1088/1748-9326/ab80f0, 2020a.

Luo, Y.C., Zhang, Z., Chen, Y., Li, Z.Y., and Tao, F.L.: ChinaCropPhen1km: a high-resolution crop phenological dataset for three staple crops in China during 2000-2015 based on leaf area index (LAI) products, Earth Syst. Sci. Data, 12, 197-214, https://doi.org/10.5194/essd-12-197-2020, 2020b.

Lv, Q.C., Yang, Z.Y., Chen, Z.Y., Li, M.C., Gao, B.B., Yang, J., Chen, X., and Xu, B.: Crop residue burning in China (2019-2021): Spatiotemporal patterns, environmental impact, and emission dynamics, Env. Sci. Ecotechnol., 21, 100394, https://doi.org/10.1016/j.ese.2024.100394, 2024.

Mehmood, K., Wu, Y.J., Wang, L.Q., Yu, S.C., Li, P.F., Chen, X., Li, Z., Zhang Y.B., Li, M.Y., Liu, W.P., Wang, Y.S., Liu, Z.R., Zhu, Y.N., Rosenfeld, D., and Seinfeld, J.H.: Relative effects of open biomass burning and open crop straw burning on haze formation over central and eastern China: modeling study driven by constrained emissions, Atmos. Chem. Phys., 20, 2419-2443, https://doi.org/10.5194/acp-20-2419-2020, 2020.

National Bureau of Statistics of China (NBSC): China Statistical Yearbook, China Statistics Press, Beijing, http://www.stats.gov.cn/sj/ndsj/, 2002-2021. (in Chinese)

Pan, X.L., Kanaya, Y., Taketani, F., Miyakawa, T., Inomata, S., Komazaki, Y., Tanimoto,

716 H., Wang, Z., Uno, I., and Wang, Z.F.: Emission characteristics of refractory black
717 carbon aerosols from fresh biomass burning: a perspective from laboratory experiments,
718 Atmos. Chem. Phys., 17, 13001-13016, https://doi.org/10.5194/acp-17-13001-2017,
719 2017.
720 Peng, L.Q., Zhang, Q., and He, K.B.: Emissions inventory of atmospheric pollutants
721 from open burning of crop residues in China based on a national questionnaire, Res.
722 Environ. Sci., 29, 1109-1118, 2016. (In Chinese)
723 Saxton, K.E., Kenny, J.F., and McCool, D.K.: Air permeability to define frozen soil
724 infiltration with variable tillage and residue, Trans. ASABE, 36, 1369-1375,
725 https://dx.doi.org/10.13031/2013.28472, 1993.
726 Schroeder, W., Oliva, P., Giglio, L., and Csiszar, I.A.: The New VIIRS 375 m active
727 fire detection data product: Algorithm description and initial assessment, Remote Sens.
728 Environ., 143, 85-96, https://dx.doi.org/10.1016/j.rse.2013.12.008, 2014.
729 Shi, W.J., Fang, Y.R., Chang, Y.Y., and Xie, G.H.: Toward sustainable utilization of crop
730 straw: Greenhouse gas emissions and their reduction potential from 1950 to 2021 in
731 China, Resour. Conserv. Recy., 190, 106824,
732 https://doi.org/10.1016/j.resconrec.2022.106824, 2023.
733 Song, Z.H., Zhang, L.M., Tian, C.G., Li, K.Y., Chen, P.Y., Jia, Z.Y., Hu, P., and Cui,
734 S.: Chemical characteristics, distribution patterns, and source apportionment of
735 particulate elements and inorganic ions in snowpack in Harbin, China, Chemosphere,
736 349, 140886, https://doi.org/10.1016/j.chemosphere.2023.140886, 2024.

737 Stavrakou, T., Müller, J.F., Bauwens, M., De Smedt, I., Lerot, C., Van Roozendael, M.,
738 Coheur, P.F., Clerbaux, C., Boersma, K.F. van der A, R., and Song, Y.: Substantial
739 underestimation of post-harvest burning emissions in the North China plain revealed
740 by multi-species space observations, Sci. Rep., 6, 32307,
741 https://dx.doi.org/10.1038/srep32307, 2016.
742 Stockwell, C.E., Yokelson, R.J., Kreidenweis, S.M., Robinson, A.L., DeMott, P.J.,
743 Sullivan, R.C., Reardon, J., Ryan, K.C., Griffith, D.W.T., and Stevens, L.: Trace gas
744 emissions from combustion of peat, crop residue, domestic biofuels, grasses, and other
745 fuels: configuration and Fourier transform infrared (FTIR) component of the fourth Fire
746 Lab at Missoula Experiment (FLAME-4), Atmos. Chem. Phys., 14, 9727-9754,
747 https://doi.org/10.5194/acp-14-9727-2014, 2014.
748 Sun, J.F., Peng, H.Y., Chen, J.M., Wang, X.M., Wei, M., Li, W.J., Yang, L.X., Zhang,
749 Q.Z., Wang, W.X., and Mellouki, A.: An estimation of CO_2 emission via agricultural
750 crop residue open field burning in China from 1996 to 2013, J. Clean. Prod., 112, 2625-
751 -2631, https://dx.doi.org/10.1016/j.jclepro.2015.09.112, 2016.
752 Syphard, A.D., Keeley, J.E., Pfaff, A.H., and Ferschweiler, K.: Human presence
753 diminishes the importance of climate in driving fire activity across the United States, P.
754 Natl. Acad. Sci. U.S.A., 114, 13750-13755, https://doi.org/10.1073/pnas.1713885114,
755 2017.
756 Tang, R., Huang, X., Zhou, D.R., and Ding, A.J.: Biomass-burning-induced surface
757 darkening and its impact on regional meteorology in eastern China, Atmos. Chem.

758 Phys., 20, 6177-6191, https://doi.org/10.5194/acp-20-6177-2020, 2020.
759 Tao, S., Ru, M.Y., Du, W., Zhu, X., Zhong, Q.R., Li, B.G., Shen, G.F., Pan, X.L., Meng,
760 W.J., Chen, Y.L., Shen, H.Z., Lin, N., Su, S., Zhuo, S.J., Huang, T.B., Xu, Y., Yun, X.,
761 Liu, J. F., Wang, X.L., Liu, W.X., Cheng, H.F., and Zhu, D.Q.: Quantifying the rural
762 residential energy transition in China from 1992 to 2012 through a representative
763 national survey, Nat. Energy, 3, 567-573, https://doi.org/10.1038/s41560-018-0158-4,
764 2018.
765 Tian, H., Zhao, D., and Wang, Y.: Emission inventories of atmospheric pollutants
766 discharged from biomass burning in China, Acta Sci. Circumstantiae, 31, 349-357, 2011.
767 (in Chinese)
768 Vadrevu, K., and Lasko, K.: Intercomparison of MODIS AQUA and VIIRS I-Band fires
769 and emissions in an agricultural landscape-implications for air pollution research,
770 Remote Sens., 10, 978, https://doi.org/10.3390/rs10070978, 2018.
771 van der Werf, G.R., Randerson, J.T., Giglio, L., van Leeuwen, T.T., Chen, Y., Rogers,
772 B.M., Mu, M.Q., van Marle, M.J.E., Morton, D.C., Collatz, G.J., Yokelson, R.J., and
773 Kasibhatla, P.S.: Global fire emissions estimates during 1997-2016, Earth Syst. Sci.
774 Data, 9, 697-720, https://doi.org/10.5194/essd-9-697-2017, 2017.
775 Vermote, E., Ellicott, E., Dubovik, O., Lapyonok, T., Chin, M., Giglio, L., and Roberts,
776 G.J.: An approach to estimate global biomass burning emissions of organic and black
777 carbon from MODIS fire radiative power, J. Geophys. Res., 114, D18
778 https://doi.org/10.1029/2008jd011188, 2009.

779 Wang, J.Y., Xi, F.M., Liu, Z., Bing, L.F., Alsaedi, A., Hayat, T., Ahmad., and Guan,
780 D.D.: The spatiotemporal features of greenhouse gases emissions from biomass burning
781 in China from 2000 to 2012, J. Clean. Prod., 181, 801-808,
782 https://doi.org/10.1016/j.jclepro.2018.01.206, 2018.
783 Wang, X.Y., Xue, S., and Xie, G.H.: Value-taking for residue factor as a parameter to
784 assess the field residue of field crops, J. China Agr. Univ., 17.1, 1-8, 2012. (in Chinese)
785 Weldemichael, Y., and Assefa, G.: Assessing the energy production and GHG
786 (greenhouse gas) emissions mitigation potential of biomass resources for Alberta, J.
787 Clean. Prod., 112, 4257-4264, https://doi.org/10.1016/j.jclepro.2015.08.118, 2016.
788 Wen, X., Chen, W.W., Chen, B., Yang, C.J., Tu, G., and Cheng, T.H.: Does the
789 prohibition on open burning of straw mitigate air pollution? An empirical study in Jilin
790 Province of China in the post-harvest season, J. Environ. Manage., 264, 110451,
791 https://doi.org/10.1016/j.jenvman.2020.110451, 2020.
792 Wiedinmyer, C., Kimura, Y., McDonald-Buller, E.C., Emmons, L.K., Buchholz, R.R.,
793 Tang, W.F., Seto, K., Joseph, M.B., Barsanti, K.C., Carlton, A.G., and Yokelson, R.:
794 The Fire Inventory from NCAR version 2.5: an updated global fire emissions model for
795 climate and chemistry applications, Geosci. Model Dev., 16, 3873-3891,
796 https://doi.org/10.5194/gmd-16-3873-2023, 2023.
797 Wiedinmyer, C., Yokelson, R.J., and Gullett, B.K.: Global emissions of trace gases,
798 particulate matter, and hazardous air pollutants from open burning of domestic waste,
799 Environ. Sci. Technol., 48, 16, 9523-9530, https://doi.org/10.1021/es502250z, 2014.

Wooster, M.J., Roberts, G., Perry, G.L.W., and Kaufman, Y.J.: Retrieval of biomass combustion rates and totals from fire radiative power observations: FRP derivation and calibration relationships between biomass consumption and fire radiative energy release, J. Geophys. Res-Atmos., 110, D24311, https://doi.org/10.1029/2005JD006318, 2005.

Wu, B.B., Li, J.H., Yao, Z.L., Li, X., Wang, W.J., Wu, Z.C., and Zhou, Q.: Characteristics and reduction assessment of GHG emissions from crop residue open burning in China under the targets of carbon peak and carbon neutrality, Sci. Total Environ., 905, 167235, https://doi.org/10.1016/j.scitotenv.2023.167235, 2023.

Wu, J., Kong, S.F., Wu, F.Q., Cheng, Y., Zheng, S.R., Qin, S., Liu, X., Yan, Q., Zheng, H., Zheng, M.M., Yan, Y.Y., Liu, D.T., Ding, S., Zhao, D.L., Shen, G.F., Zhao, T.L., and Qi, S.H.: The moving of high emission for biomass burning in China: View from multi-year emission estimation and human-driven forces. Environ. Int., 142, 105812, https://doi.org/10.1016/j.envint.2020.105812, 2020.

Wu, J., Kong, S.F., Wu, F.Q., Cheng, Y., Zheng, S.R., Yan, Q., Zheng, H., Yang, G.W., Zheng, M.M., Liu, D.T., Zhao, D.L., and Qi, S.H.: Estimating the open biomass burning emissions in central and eastern China from 2003 to 2015 based on satellite observation, Atmos. Chem. Phys., 18, 11623-11646, https://doi.org/10.5194/acp-18-11623-2018, 2018.

Xu, R.B., Ye, T.T., Yue, X., Yang, Z.Y., Yu, W.H., Zhang, Y.W., Bell, M.L., Morawska, L., Yu, P., Zhang, Y.X., Wu, Y., Liu, Y.M., Johnston, F., Lei, Y.D., Abramson, M.J., Guo,

821 Y.M., and Li, S.S.: Global population exposure to landscape fire air pollution from 2000
822 to 2019, Nature, 621, 521-529, https://doi.org/10.1038/s41586-023-06398-6, 2023a.
823 Xu, C., and You, C.: Agricultural expansion dominates rapid increases in cropland fires
824 in Asia, Environ. Int., 179, https://doi.org/108189, 10.1016/j.envint.2023.108189,
825 2023b.
826 Xu, W.D., Wooster, M.J., Kaneko, T., He, J.P., Zhang, T.R., and Fisher, D.: Major
827 advances in geostationary fire radiative power (FRP) retrieval over Asia and Australia
828 stemming from use of Himarawi-8 AHI, Remote Sens. Environ., 193, 138-149,
829 https://dx.doi.org/10.1016/j.rse.2017.02.024, 2017.
830 Xuan, F., Dong, Y., Li, J.Y., Li, X.C., Su, W., Huang, X.D., Huang, J.X., Xie, Z.X., Li,
831 Z.Q., Liu, H., Tao, W.C., Wen, Y.A., and Zhang, Y.: Mapping crop type in Northeast
832 China during 2013-2021 using automatic sampling and tile-based image classification,
833 Int. J. Appl. Earth Obs., 117, 103178, https://doi.org/10.1016/j.jag.2022.103178, 2023.
834 Yang, G.Y., Zhao, H.M., Tong, D.Q., Xiu, A.J., Zhang, X.L., and Gao, C.: Impacts of
835 post-harvest open biomass burning and burning ban policy on severe haze in the
836 Northeastern China, Sci. Total Environ., 716, 136517,
837 https://doi.org/10.1016/j.scitotenv.2020.136517, 2020.
838 Yang, Y., and Zhao, Y.: Quantification and evaluation of atmospheric pollutant
839 emissions from open biomass burning with multiple methods: a case study for the
840 Yangtze River Delta region, China, Atmos. Chem. Phys., 19, 327-348,
841 https://doi.org/10.5194/acp-19-327-2019, 2019.

Ying, L.X., Shen, Z.H., Yang, M.Z., and Piao, S.L.: Wildfire detection probability of modis fire products under the constraint of environmental factors: A study based on confirmed ground wildfire records, Remote Sens., 11, 24, 3031, https://doi.org/10.3390/rs11243031, 2019.

Zhang, X.H., Lu, Y., Wang, Q.G., and Qian, X.: A high-resolution inventory of air pollutant emissions from crop residue burning in China, Atmos. Environ., 213, 207-214, https://doi.org/10.1016/j.atmosenv.2019.06.009, 2019.

Zhang, T.R., de Jong, M.C., Wooster, M.J., Xu, W.D., and Wang, L.L.: Trends in eastern China agricultural fire emissions derived from a combination of geostationary (Himawari) and polar (VIIRS) orbiter fire radiative power products, Atmos. Chem. Phys., 20, 10687-10705, https://doi.org/10.5194/acp-20-10687-2020, 2020.

Zhao, H.M., Yang, G.Y., Tong, D.Q., Zhang, X.L., Xiu, A.J., and Zhang, S.C.: Interannual and seasonal variability of greenhouse gases and aerosol emissions from biomass burning in Northeastern China constrained by satellite observations, Remote Sens., 13, 1005, https://doi.org/10.3390/rs13051005, 2021.

Zheng, B., Ciais, P., Chevallier, F., Yang, H., Canadell, J.G., Chen, Y., van der Velde, I.R., Aben, I., Chuvieco, E., Davis, S.J., Deeter, M., Hong, C.P., Kong, Y.W., Li, H.Y., Li, H., Lin, X., He, K.B., and Zhang, Q.: Record-high CO_2 emissions from boreal fires in 2021, Science, 379, 912-917, https://doi.org/10.1126/science.ade0805, 2023.

Zhou, Y., Xia, X.C., Lang, J.L., Zhao, B.B., Chen, D.S., Mao, S.S., Zhang, Y.Y., Liu, J., and Li, J.: A coupled framework for estimating pollutant emissions from open burning

863 of specific crop residue: A case study for wheat, Sci. Total Environ., 844, 156731,
864 https://doi.org/10.1016/j.scitotenv.2022.156731, 2022.
865 Zhou, Y., Xing, X.F., Lang, J.L., Chen, D.S., Cheng, S.Y., Wei, L., Wei, X., and Liu, C.:
866 A comprehensive biomass burning emission inventory with high spatial and temporal
867 resolution in China, Atmos. Chem. Phys., 17, 2839-2864, https://doi.org/10.5194/acp-
868 17-2839-2017, 2017.
869 Zhuang, Y., Li, R.Y., Yang, H., Chen, D.L., Chen, Z.Y., Gao, B.B., and He, B.:
870 Understanding temporal and spatial distribution of crop residue burning in China from
871 2003 to 2017 using MODIS data, Remote Sens., 10(3), 390,
872 https://doi.org/10.3390/rs10030390, 2018.
873 Zhu, C., Kawamura, K., and Kunwar, B.: Effect of biomass burning over the western
874 North Pacific Rim: Wintertime maxima of anhydrosugars in ambient aerosols from
875 Okinawa, Atmos. Chem. Phys., 15, 1959-1973, https://doi.org/10.5194/acp-15-1959-
876 2015, 2015.